CaIN: Low Power and Low Latency VHF Mesh Networking

Mengyao Liu
mengyao.liu@kuleuven.be
DistriNet, KU Leuven
3001 Leuven, Belgium

Bingwu Fang
bingwu.fang@kuleuven.be
DistriNet, KU Leuven
3001 Leuven, Belgium

Jonathan Oostvogels
jonathan.oostvogels@kuleuven.be
DistriNet, KU Leuven
3001 Leuven, Belgium

Sam Michiels
sam.michiels@kuleuven.be
DistriNet, KU Leuven
3001 Leuven, Belgium

Andrei Belogaev
andrei.belogaev@uantwerpen.be
IDLab, University of Antwerp–imec
Antwerpen, Belgium

Xinlei Liu
xinlei.liu@uantwerpen.be
IDLab, University of Antwerp–imec
Antwerpen, Belgium

Jeroen Famaey
jeroen.famaey@uantwerpen.be
IDLab, University of Antwerp–imec
Antwerpen, Belgium

Danny Hughes
danny.hughes@kuleuven.be
DistriNet, KU Leuven
3001 Leuven, Belgium

Abstract

Low-power wireless mesh networks provide a solution for the seamless wireless coverage of complex physical environments due to their ability to route around physical obstructions and sources of interference. For example, networks such as SmartMesh-IP, WirelessHART and 6TiSCH deliver industry-grade reliability with low routing power consumption. However, conventional low power mesh networks suffer from high latency. The root of this problem is the need to reduce receiver power consumption by duty cycling the radio receiver using time-synchronized wake-ups or preamble sampling. We tackle this problem by introducing *CaIN*, a near field mesh network that transmits information using strong Capacitive and INductive effects that can be detected by a passive receiver front end, thereby side-stepping the need for intermittent receiver usage. Given that near field effects are limited to a few wavelengths, we implement our proof-of-principle transceiver in the VHF frequency band at 40 MHz, achieving a unique performance profile including: 20 kbps link layer throughput, sub-μW receiver power consumption, sub-ms wireless wake-up and 17 m per-hop range. Building upon these properties, we realize a novel mesh network with a worst-case latency of under 40 ms for a 3 hop network. To promote replication and further work, we have made the hardware and software of our reference implementation open source.

CCS Concepts

• **Networks** → **Physical links**; **Network design principles**; **Sensor networks**.

Keywords

Near field wireless mesh networking, low latency networking, ultra low power receiver design

1 Introduction

Low power Wireless Mesh Networks (WMN) are an essential part of the wireless communication landscape. By implementing routing functionality on top of short-range radios such as IEEE 802.15.4 or Bluetooth Low Energy, it is possible to realize an extensible wireless fabric that can cover challenging physical environments such as vehicles, factories and buildings without the need to deploy large numbers of powered gateways. WMN technologies have a proven track record of delivering high end-to-end reliability while preserving multi-year battery life [6, 38, 39].

Current WMN radios alternate between low-power states in which they cannot receive data and more power-hungry states in which they can. Such duty cycling is necessary to reconcile their power consumption in receive mode (several mW) with the average energy budget available over multiple years (tens of µW). As data can only be communicated if a transmitter and a receiver agree on when to do so, WMNs coordinate rendezvous points, for example by synchronising wake-ups in time [38, 39], or by preamble sampling [4, 28]. Such duty-cycled rendezvous increases end-to-end latency for aperiodic or event-driven traffic, which often scales to many seconds for large mesh networks. This precludes the use of these technologies in time-sensitive applications.

The core scientific contribution of this paper is to introduce the paradigm of *near field mesh networking*, a novel approach to low power and low latency networking. While the near field is limited in range to a few wavelengths due to its reliance on capacitive and inductive effects, those effects are dramatically stronger than the far field. This higher received signal strength simplifies transceiver design, enabling sub-microwatt power consumption in receive mode. Near-field communication has a long track record in the form of Radio Frequency ID (RFID) [21], though the range of RFID is limited to a few meters even with powerful transmitters and directional antennas. CaIN addresses this range limitation with a two-fold approach; firstly by operating at VHF frequencies to maximize near-field range and secondly building a WMN to enable the coverage of larger areas.

The proposed paradigm is supported by two engineering contributions; (i.) an open source hardware and software reference design, that enables further experimentation with near-field mesh networking (https://github.com/KULeuvenNESLFradio/CaIN) and (ii.) a systematic evaluation of the approach in real-world conditions. The current prototype of CaIN operates between 20 MHz and 80 MHz. This carrier wave is modulated using On/Off Keying (OOK) and Manchester coded. The frequency of the carrier wave

is configurable in software and may be tailored to suit the specific environment and available frequency bands.

CaIN offers a unique and complementary performance profile in comparison to Radio Frequency ID (RFID), 802.15.4 and Bluetooth Low Energy (BLE). Its ultra low receiver power enables always-on operation, thereby eliminating the latency that arises in mesh networks due to receiver duty cycling. Furthermore, reasonable transmitter power consumption together with omni-directional antennas enable the construction of a multi-hop wireless mesh with dramatically lower end-to-end latency than previous approaches.

The remainder of this paper is structured as follows. Section 2 provides background on radio duty cycling, active wakeup and near field communication. Section 3 then describes the design of the CaIN transceiver and network stack. Section 4 describes key implementation details. Section 5 evaluates the reference implemetation of CaIN in realistic network scenarios. Section 6 discusses related work. Section 7 concludes. Finally, Section 8 discusses promising directions for future work.

2 Background

Section 2.1 to 2.3 provide background on key themes related to CaIN, including radio duty cycling, always-on low-power radios, and near field communication. Section 2.4 then identifies requirements for the design of CaIN.

2.1 Radio Duty Cycling

Conventional radios use significant power when listening for incoming transmissions and must therefore be duty cycled in order to maintain an acceptable power profile. Two archetypal approaches have emerged to managing radio duty cycles and rendezvous: preamble sampling and time synchronization.

2.1.1 Preamble Sampling. With preamble sampling [28], one of a pair of devices announces its intent to communicate data by transmitting a bit pattern of length L in time, while the other device samples the channel at a rate of R, where $R \leq L$. Preamble sampling enables the receiver to be duty cycled at the expense of additional power consumption and latency for the sender. Longer preambles will result in lower power consumption for receivers at the expense of latency. Similarly, *low-power probing* [22] approaches have receivers announce their willingness to receive data, thus also reducing spurious listening at the expense of latency.

2.1.2 Time Synchronization. Time Synchronized Network (TSN) protocols such as 6TiSCH [38] schedule per-node transmit and receive slots and thereby eliminate the need for preamble sampling and further reduce power consumption. However, latency is increased for unpredictable traffic flows, as transmitters must wait for a scheduled transmit slot before they are able to send. In the case of multi-hop mesh networks, this latency scales with the diameter of the network, often to several seconds.

2.2 Wake-up Radios

Wake-up Radios (WuRs) are a class of always-on, ultra low power radio designs. As this class of radios are considerably less sensitive than their more power consuming counterparts, they are typically used to communicate a special-purpose wake-up signal that initiates subsequent communication using a conventional primary radio [26]. For the same reason, WuRs often depend on relatively powerful transmitters [26]. Since a WuR is always on, latency can be reduced in comparison to the RDC approaches discussed in Section 2.1. This paper demonstrates that WuR-like radio design, when combined with VHF communication and near-field meshed deployments, enables considerable improvements to the latency-energy trade-off encountered in low-power networks.

WuRs operating in the μW range share many common design elements, being based around envelope detectors, passive voltage multiplication and digital comparators to demodulate an On/Off Keyed (OOK) wake-up signal. For instance, Bdiri et al. [2] introduce a 868 MHz receiver, which achieves a range of 2.5 m, data rate of 1.2 kbps and a power consumption of 690 nW. A CC1101[1] transmitter is used to send the wake-up signal consuming 74 mW. Marinkovic et al. [19] introduce a 433 MHz WuR, which achieves a range of 10 m, a data rate of 5.5 kbps and a power consumption of 270 nW. An ADI ADF7020[2] was used to provide a wake-up signal, consuming 85 mW. Magno et al. [17] introduce an 868 MHz WuR which achieves a range of up to 50 m, a data rate of 10 kbps and receiver power of 1.2 μW. A TI CC430F614x[3] provides the wake-up signal, consuming 105 mW. For a complete review of wake-up radios, we refer the reader to Piyare et al. [26].

2.3 Radio Frequency ID

Radio Frequency ID (RFID) is designed to support simple and low cost *tags* that may be read and written at short range by a powerful *reader*. In the case of *passive* tags (i.e. battery free), Wireless Power Transfer (WPT) from the receiver is used to provide all operastional energy. RFID is available in a range of frequencies: LF (135 kHz), HF (13.5 MHz) and UHF (868/915 MHz). Near Field Communication (NFC) is a strict subset of the HF RFID variant [21].

LF and HF tags depend upon the strong coupling effects that occur within the *near field* and offer ranges between a few centimeters and a few meters, while UHF tags, for example the WISP platform [30], depend upon the far field effect and offer operational rages of around 3 meters using a conventional reader. RFID tags typically communicate using *backscatter*, modifying the properties of their antenna to selectively reflect the incident signal from the receiver and thereby transmit a response to the reader at orders of magnitude less power than an active radio. While RFID offers a simple and low power solution to communication, it is inherently short range and due to the requirement for a powerful reader, typically operating at 10s of dBm and consuming multiple Watts, RFID is limited to star topologies and cannot practically be meshed.

2.4 Requirements

The overall goal of CaIN is to enable the construction of low latency mesh networks at ultra low power. This leads to three technical requirements:

(1) **Ultra Low Power Receiver:** RDC inevitably increases per-hop latency. An ultra low power always-on receiver is

[1] CC1101 Datasheet
[2] ADF7020 Datasheet
[3] TI CC430F614x Datasheet

required which does not add significantly to the deep sleep current of a conventional MCU (order of 1 μW).

(2) **Integrated Transceiver Design:** The low data rate and high transmitter power of conventional WuR requires the use of a separate radio for wake-up and communication, increasing size and design complexity. An integrated transceiver is required which supports both sub-μW listening and similar end-to-end data rates to conventional radios (order of 10 kbps).

(3) **Transmitter Range** must also be maximized to preserve freedom in deploying and designing mesh networks. This also precludes the use of directional antennas as is common in RFID. Specifically we aim for an omnidirectional range of at least several meters.

In the following chapter we elaborate on the design of CaIN, a system which fulfils these requirements.

3 System Design

In this section, we describe the design of CaIN. Section 3.1 describes the physical layer design of CaIN, while Section 3.2 describes the CaIN data link layer, Together these two layers are sufficient to realize a simple single-controller wireless bus. The higher layers of the protocol stack, from Network to Transport are the subject of future work, as discussed in Section 7.

3.1 Physical Layer

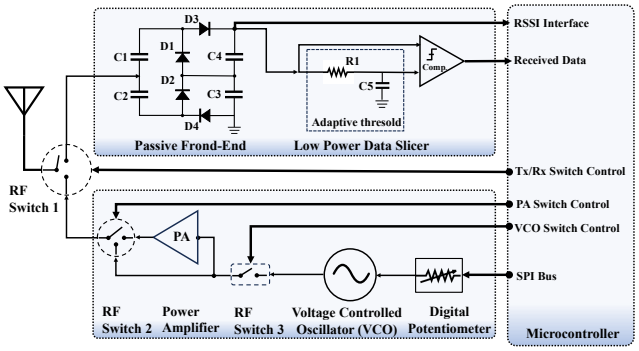

Figure 1: High-level block diagram of a CaIN transceiver.

The physical layer design of CaIN is illustrated in the block diagram of Figure 1. The receiver and transmitter are described in Section 3.1.1 and 3.1.2 respectively.

3.1.1 Transmitter. CaIN takes a very simple approach to transmitting data, which in turn enables the creation of a nearly-passive receiver. A Voltage Controlled Oscillator (VCO) generates a Very High Frequency (VHF) carrier wave in the range of 20 to 80 MHz. This enables access to three unlicensed frequency bands at 27, 35 and 40 MHz[4]. Certification in one of these frequency bands will be the subject of our future work as described in Section 8. The frequency of the VCO is selected by the application MCU via a digital potentiometer connected to the Serial Peripheral Interface (SPI) bus. The application MCU controls switching between receive and transmit modes via RF Switch 1. The output of the VCO may be amplified by a *Power Amplifier (PA)* which is controlled by RF switch 2. Data is modulated by On/Off Keying (OOK) the VCO output using a RF Switch 3. Experimentation has shown that data rates of up to 4.9kbps are achievable without amplification and 19.8kbps with the amplifier active.

3.1.2 Receiver. The key challenge for the receiver is to mimimize power consumption while amplifying the received signal to the point that it can be used to demodulate OOK data. CaIN accomplishes this using a passive front-end and a low-power data slicer.

Passive front end: The CaIN front-end is based on a Greinacher voltage multiplier, which rectifies the received signal and increases its voltage to a usable level. This is a common design in passive RF front ends such as those found in WuR [26] and in Wireless Power Transfer (WPT) systems [36]. By building our transceiver in the VHF frequency range, we side-step much of the optimization complexity that is typical in passive and ultra low power receivers in the UHF and ISM* bands (868MHz and 2.4GHz). At ranges of up to a few wavelengths (7-30 m for the transmitter described in Section 3.1.1), near field coupling effects result in a strong received signal strength even at modest transmit power. The Greinacher voltage multiplier operates as a capacitive charge pump circuit. The optimal capacitance value can be calculated using the following formula:

$$C = \frac{I \cdot T}{\Delta V} \tag{1}$$

Where C is the size of the capacitors in the voltage multiplier, I is the load current, T is the period of the received waveform and ΔV is the minimal voltage swing that is necessary to overcome the internal hysteresis of the low-power data slicer. In practice, capacitors may be selected slightly above the calculated values to provide a buffer against sub-optimal conditions. As can be seen from Equation 1, high carrier frequencies (supporting fast symbol rates) demand low capacitance, whereas lower carrier frequencies (offering extended range) necessitate higher capacitance. In the current prototype of CaIN, these components are manually tailored to match the carrier frequency.

Low-power data slicing: Conventional radios use high-speed (and therefore high-power) Analogue-to-Digital Converters (ADCs) to demodulate the received signal. However, the low power data slicing module of CaIN takes a different approach, using an sub-μW comparator to threshold the analogue signal and thereby convert it into a series of symbols. An RC low pass filter is applied to one of the comparator's inputs to support dynamic thresholding of the input signal and increase immunity against background noise [20]. As with the passive front end, the values of R1 and C5 are tailored to suit CaIN's symbol rate as described by Equation 2 below:

$$f_c = \frac{1}{2\pi RC}. \tag{2}$$

f_c is the filter's cutoff frequency, which we set to 330 Hz, well above common sources of AC interference, but well below CaIN's minimal data rate. The output of the data slicer is provided to the CaIN data link layer running on the application MCU. In the current version

[4]https://transition.fcc.gov/oet/spectrum/table/fcctable.pdf

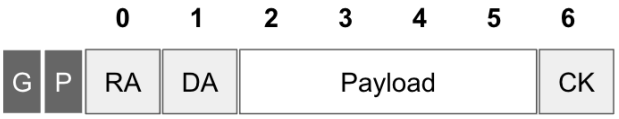

Figure 2: CaIN's 7 Byte Frame Structure

of CaIN, the values of analog components in the passive front-end and data slicer are fixed. However, dynamically tuning them forms part of our future work as described in Section 8.

3.2 Data Link Layer

The CaIN data link layer implements a simple single controller addressable bus structure. That is, a single controller device initiates all traffic by transmitting a request to some other device. That request is then routed through the network across multiple hops until it reaches it destination. Next, the destination node generates a reply packet, which is then routed in the opposite direction, i.e. towards the controller node.

3.2.1 Symbol Coding. CaIN encodes binary data using Differential Manchester coding, wherein each bit is represented by a transition or a lack thereof in the signal. This approach provides synchronization, noise immunity and a degree of error resilience. The self-clocking character of Manchester coding is a good fit with CaIN, wherein the receiver must decode data encoded at different data rates (from 4.9 to 19.8 kbps).

3.2.2 Frame Structure. The data link layer frame format of CaIN is shown in Figure 2, wherein:

- **G** is 0.8ms (4b) of dead-time used to delineate packets.
- **P** is 0.8ms (4b) of preamble to wake the receiver.
- **RA** is an 8b Receiver Address for the next hop.
- **DA** is an 8b final Destination Address.
- **Payload** is 32b of freeform application data.
- **CRC** is an 8b checksum to detect corrupt packets.

This small packet structure is heavily optimized for low latency operation, enabling CaIN to maximally exploit latency gains arising from its always-on receiver. As we implement a single-controller bus, no source address is required.

3.2.3 Forwarding. The forwarding behaviour of CaIN is simple. At each hop, the receiver RA will first validate checksum CK, discarding corrupted packets. If the packet is intact, a lookup is performed on RAs routing table for the destination address DA. If DA is known, a new packet is then generated and retransmitted to the next hop on the route to DA. As the current version of CaIN implements a unicast single-controller bus, there is no source of contention, though interference may occur from co-located RF sources.

CaIN does not tackle the problem of finding and disseminating routes accross the network. For the purposes of the mesh experiments performed in this paper, multi-hop routes are known a-priori. In our future work we will investigate how existing approaches such as the Routing Protocol for Low-Power and Lossy Networks (RPL) [40], 6TiSCH [38] and Ad-Hoc On Demand Distance Vector (AODV) [24] can be applied for static and mobile scenarios respectively.

4 Implementation

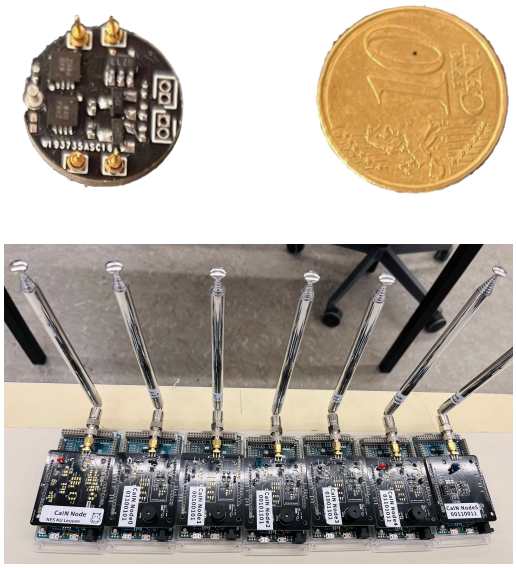

Figure 3: CaIN transceiver prototype (16 mm diameter, top) and the evaluation boards with antenna (bottom).

This section describes a prototypical implementation of CaIN, relying on a embedded microcontroller to control the low-power radio front-end under test. All source code and hardware designs are available at(https://github.com/KULeuvenNESLFradio/CaIN) .

4.1 Software

The CaIN transceiver has minimal requirements of the Application MCU. In terms of IO, CaIN requires an SPI connection to the Transmitter and three General Purpose IO (GPIO) pins to switch the transceiver mode, send and receive data. The application MCU also hosts the CaIN data link layer.

Following initialization, the MCU uses the RF switch that connects the antenna to the receiver front-end to place the transceiver into receive mode. the MCU may then attach an interrupt handler to the RX pin and enter sleep mode, ready to be activated by a received CaIN message. Once awake in receive mode, the MCU will access the digital symbol stream from the data slicer to decode incoming packets. As the receiver is always on, yet consuming very little power, the need for RDC is eliminated.

When acting as a transmitter, the transceiver's MCU activates the RF switch via GPIO and connects the antenna to the transmitter's front end. The MCU fine-tunes the oscillator frequency by adjusting a digital potentiometer. Data may then be modulated by using the TX pin to toggle the RF switch, thereby modulating the carrier frequency for signal transmission. Transmit power and maximum symbol rate can be increased by activating the embedded amplifier (from 4.9 to 19.8 kbps). We believe that efficiency and simplicity can

be further improved by moving the full implementation of CaIN to a dedicated transceiver module offering a packet-based interface. This will be a subject of our future work.

4.2 Hardware

The current version of CaIN is shown in Figure 3 and matches the footprint of an *Arduino shield* enabling easy prototyping with a wide range of application MCUs. The hardware Bill of Materials for the CaIN transceiver along with the component cost in units of 10K is shown in Table 1 below. This excludes both the application MCU and antenna, as we expect these to be customised based on the needs of the application.

Table 1: Bill of Material (BoM) for the CaIN transceiver prototype in 10K order volumes

CaIN Prototype Components	Part Number	Price @10K (USD)
Rectifying Diodes	SMS7630-005LF	0.57
RF SPDT Switches	ADG918	2.46
RF SPST Switch	ADG902	1.49
Analog Comparator	TLV7031	0.173
VCO	LTC6905	1.15
RF Amplifier	TRF37D73	0.43
Resistors and Capacitors	NA	0.23
Antenna Connector	SMA-EDGE-S	1.59
Total		**8.093**

As can be seen from Table 1, even when fabricated from discrete components, the cost of a CaIN transceiver is low. As no exotic components are required, it should be possible to realise a future design of CaIN as a miniaturised System on Module at a significantly lower price point.

5 Evaluation

This section evaluates the performance of CaIN. Section 5.1 first provides basic peformance data for the transceiver. Section 5.2 then evaluates the point-to-point performance of CaIN for a pair of nodes. Section 5.3 evaluates CaIN in mesh topologies. In Section 5.4, we use simulation to compare CaIN against conventional low power radios such as BLE and 802.15.4. Finally, in Section 5.5, we discuss the limitations of our approach and current prototype.

5.1 Transceiver Characteristics

The performance characteristics of the CaIN transceiver are shown in Table 2. CaIN listens for incoming messages with a power consumption of 558 nW. On receiving a message, the application MCU wakes from sleep mode in under 0.8 ms. In this mode it is capable of receiving data at rates between 4.9 kbps and 19.8 kbps. At 4.9 kbps packet reception takes 6.8 nJ, while at 19.8 kbps, it takes only 1.67 nJ, several orders of magnitude lower than a conventional radio.

The transmitter has two power settings, 23.5 mW which supports a data rate of 4.9 kbps and consumes a total of 286 μJ per transmission and 201.7 mW, which supports a data rate of 19.8 kbps and consumes a total of 609 μJ per transmission; roughly equivalent to conventional PAN and LPWAN radios respectively.

Table 2: CaIN Transceiver Characteristics

Metric	CaIN @5 Kbps	CaIN @20 Kbps
Throughput		
Avg. packet speed	4.92 Kbps	19.8 Kbps
Timings		
Preamble latency	0.80 ms	0.20 ms
Packet transmit	11.39 ms	2.82 ms
Total on-air time	12.19 ms	3.02 ms
Power Draw		
RX Passive	558 nW	558 nW
TX power	23.5 mW	201.7 mW
Energy		
RX Packet	6.802 nJ	1.685 nJ
TX Packet	286 μJ	609 μJ

Table 3 provides detailed timing characteristics for the CaIN transceiver in its 4.9 kbps and 19.8 kbps modes. As can be seen from the table, CaIN enables wireless wake-up in under 0.8 ms and address matching in as little as 1.61 ms. This enables the application MCU to remain in deep sleep mode while being responsive to incoming messages. Furthermore, as address matching can be performed in under 2 ms, nodes can return to deep sleep mode quickly in cases where they are awakened by a message that was not intended for them.

Table 3: CaIN Transceiver Timings

CaIN Mode	@ 5 Kbps	@ 20 Kbps
Preamble Delay	0.8 ms	0.2 ms
Address Match	1.61 ms	0.40 ms
Payload Send	9.78 ms	2.42 ms
Switching Time	10.60 μs	11.81 μs
Total	12.19 ms	3.02 ms

5.2 Pairwise Performance

This section evaluates the performance of a single CaIN transceiver pair in terms of range, speed, and reliability.

5.2.1 Range. Figure 4 shows the strength of the received signal in mV along with the noise floor for a receiver at distances of 1 to 15 m from the transmitter with carrier frequencies of 20, 40 and 80 MHz. All experiments were conducted outdoors in a suburban setting with a transceiver height of 2 m using a 1.2 m telescopic monopole antenna. Each data point was recorded 10 times and the results were averaged.

The figure embodies a trade-off between the range of the near field, which decreases linearly with frequency and the sub-optimality of our 1.2 m antenna, which performs increasingly poorly at lower frequencies. For this hardware configuration, 40 MHz provides

the most attractive trade-off between range and received signal strength, remaining well above the noise floor at a distance of 15 m. We therefore use a 40 MHz carrier for the remainder of this evaluation. Achievable range also depends upon required reliability and transmitter power, as will be explored in the following section.

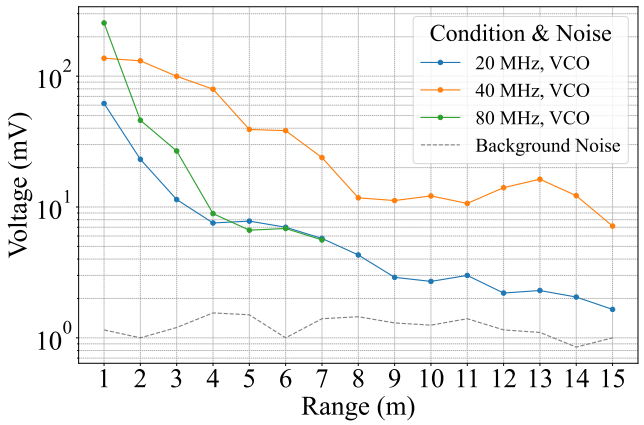

Figure 4: Received signal strength for a pair of transmitters at 20, 40 and 80 MHz and distances of 1 to 15 m.

5.2.2 Reliability. Figure 5 shows CaIN's Packet Delivery Ratio (i.e. the % of successfully received packets) for increasing packet sizes from 4 to 8B with increasing range between the transmitter and receiver. The experiments are executed twice using the two power settings and speeds of the CaIN receiver 201.7 mW / 19.8 kbps and 23.5 mW / 4.9 kbps.

As can be seen from the figure, PDR at first falls gradually with distance (until 10 m at 23 mW and 17 m at 202 mW), after which it drops precipitously to zero. This is as expected for near-field communication which is inherently limited in range. Naturally, small packets result in the highest PDR as there is less opportunity for bit-flips to occur.

Until the limit of near field communication, there is a trade-off between range and reliability. In line with current radios, we aim for a base-level of 75% PDR, resulting in an effective range of 7 m at 23 mW and 17 m at 202 mW.

5.3 Multi-Hop Performance

This section evaluates the performance of multi-hop networks of CaIN transceivers in terms of densification (Section 5.3.1) and latency (Section 5.3.2).

5.3.1 Impact of Density. For near-field communication, the number of receivers *near* the transmitter affects signal strength due to coupling. For every extra node that is placed between a transmitter and receiver, a notable drop in received signal strength occurs. In conventional wireless mesh networks, which rely on radiative power transfer rather than near-field coupling, such effects of deployment density on signal strength do not occur. "We illustrate the node topology in Figure 6, while the relationship is quantified in Figure 7. We analyse (i.) a receiver that is part of an increasing number of nodes positioned at even angles along a circular arc

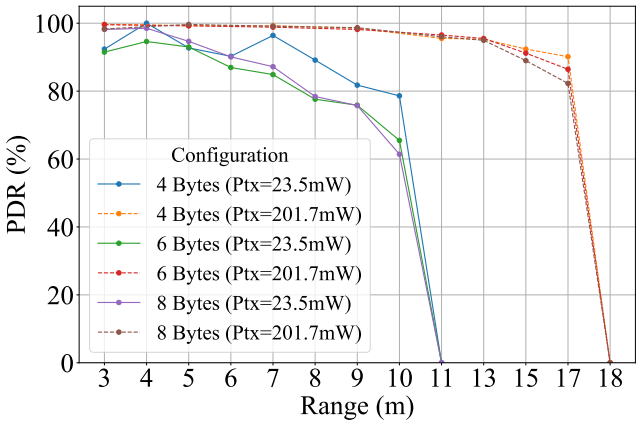

Figure 5: Packet Delivery Ratio (PDR) for packets of 4, 6 and 8B at a range of 1 to 18 m.

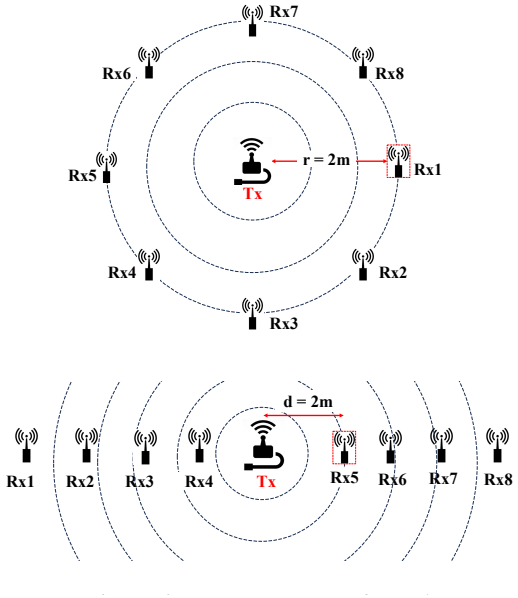

Figure 6: Receiver density topologies with 2-metre spacing: (i) Circular topology (top) and (ii) Linear topology (bottom).

corresponding to a 2-metre transmission range, and (ii.) a receiver that is part of a line of nodes spaced 2 metres apart, thus studying how signal strength evolves as deployment density increases.

As can be seen from Figure 7, signal strength is a decreasing function of deployment density surrounding the transmitter, but the maximum effect is 18% as the deployment evolves from a minimally to a maximally dense scenario, and that it decreases by no more than a few millivolts with every additional node. Interpreted in the context of Figure 4, the impact of the maximally dense deployment scenario on signal strength hence is dramatically smaller than that of positioning the transmitter-receiver pair merely one more metre

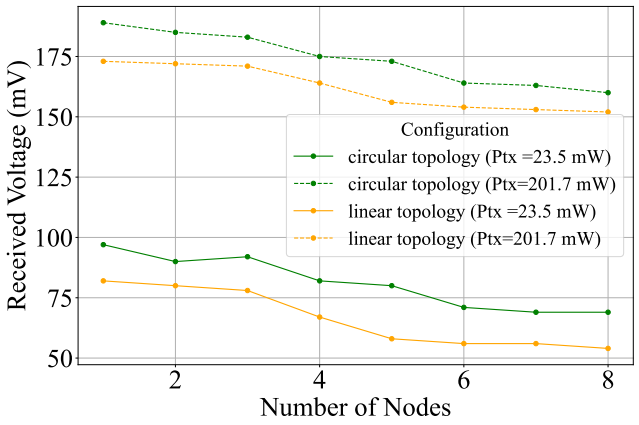

Figure 7: Network densification affects signal strength due to near-field coupling, though impacts are manageable.

apart. In mesh deployments, this adverse effect would easily be offset by the reduction in transmission distance that occurs due to a denser deployment.

5.3.2 Mesh Latency. Figure 8 evaluates the latency of a network of two to four nodes (i.e. one to three hops) deployed in a line topology with a spacing of 2 m between each node. 600 packets were transmitted for each data point.

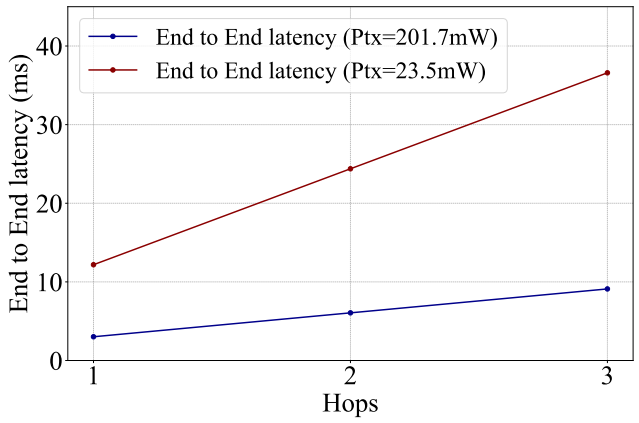

Figure 8: End-to-end latency across 1 to 3 hops.

As the single controller bus implemented by CaIN has no contention, the observed results are deterministic, matching the timings provided in Table 3 and scaling linearly with hop-count as expected. It is important to note however that, unlike conventional networks such as SmartMeshIP [39] or Bluetooth Low Energy[5], the CaIN receiver is always on and does not need to be duty-cycled. In the following section we compare the performance of CaIN to representative contemporary radios under different duty cycle settings.

[5]https://www.bluetooth.com/learn-about-bluetooth/tech-overview/

5.4 Comparison to Contemporary Radios

In this section, we use the measured performance profile of CaIN together with manufacturer provided data for two state-of-the-art low power wireless network chips.

SmartMesh IP (SMIP): The LTC5800-IPM from Analog Devices[6], is an 802.15.4 transceiver that implements TSMP [39], a 6TiSCH-like [38] time-synchronized mesh network. This radio has a base data rate of 250 kbps, 7.25 ms TX/RX slot length and supports packets of up to 128B. It consumes an average of 1.6 mW during an active receive slot and 1.96 mW during a transmit slot. All performance numbers were drawn from the data sheet.

Bluetooth Low Energy (BLE): The nRF52840 from Nordic Semiconductor[7] is a BLE transceiver. We used a base data rate of 1Mbps, 3.33 ms TX/RX slot lengths, and packets of 32B. This radio consumes an average of 1.2 mW during both TX and RX slots. Performance data was drawn from the Nordic BLE power estimator tool[8].

In the sub-sections that follow, we will first evaluate the latency bounds of these transceivers at 100% duty cycle in Section 5.4.1. We will then explore the degree to which these transceivers must be duty cycled to achieve CaIN-like power consumption in Section 5.4.2. Two major simplifying assumptions are made (i.) SMIP and BLE are perfectly scheduled by a zero-cost time-synchronisation algorithm and (ii.) arbitrarily low duty cycles are possible for SMIP and BLE. These assumptions mean that our simulations slightly overestimate the performance of conventional radios. Nevertheless, the performance of CaIN remains compelling.

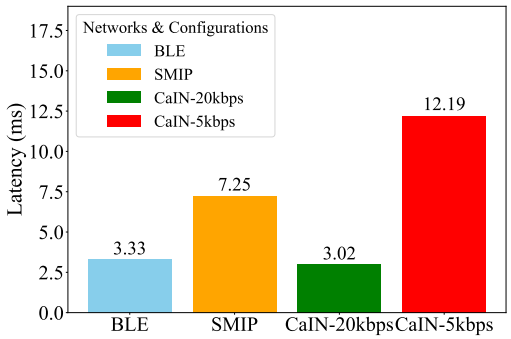

Figure 9: Latency for CaIN vs SOTA radios at 100% duty cycle.

5.4.1 Low Latency Operation. Figure 9 plots the lower bound on latency for BLE, SMIP and CaIN. For BLE and SMIP this requires a 100% duty cycle, while the CaIN receiver is always-on throughout the experiments. As can be seen from the figure, CaIN is competitive with these protocols in terms of latency even at 100% duty cycle offering a latency of 3.02 ms at 19.8 kbps and 12.19 ms at 4.9 kbps. However, this arises in large part due to CaIN's smaller 7B packet size, versus 32B for BLE and 128B for SMIP.

The key difference between CaIN and contemporary low power wireless radios becomes apparent in Figure 10 which shows the power consumption for all technologies at 100% duty cycle. As can

[6]LTC5800-IPM Datasheet
[7]nRF52840 Product Specification
[8]Nordic Power Profiler Tool

be seen from the figure, the power consumption of SMIP and BLE dwarfs that of CaIN by several orders of magnitude.

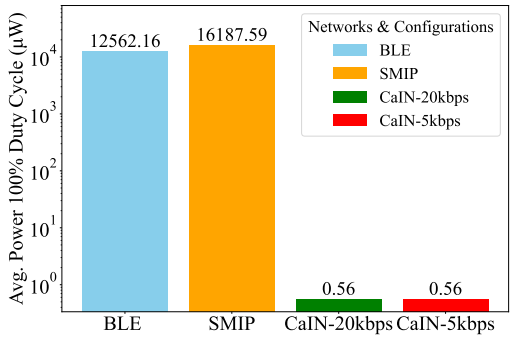

Figure 10: Average power consumption for SOTA radios and CaIN at 100% duty cycle.

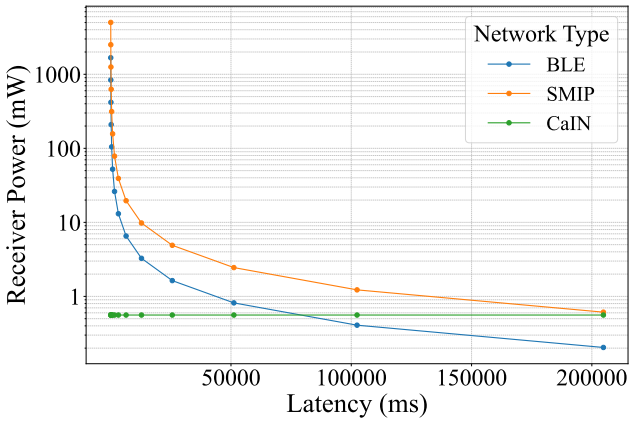

Figure 11: The relationship between receiver power and latency with increasing duty-cycles for CaIN and SoTA low power wireless radios.

Considering Figures 9 and 10 together, it becomes apparent that CaIN offers an excellent power/latency trade-off irrespective of packet size. In the follow section, we explore the degree to which SoTA transcievers can be duty-cycled to achieve CaIN-like power numbers.

5.4.2 Duty Cycled Operation. Figure 11 visualises the relationship between average receiver power consumption and duty cycle. As the different transceivers in our evaluation have different slot lengths, period (i.e. latency) is used in place of duty cycle. As can be seen from the figure, BLE power consumption converges with a CaIN receiver for a duty cycle period of around 100 seconds, while SMIP power consumption converges for a duty cycle period of around 200 seconds. This is orders of magnitude longer than CaIN's worst case latency of 12 ms. We believe that this makes a strong case for CaIN in scenarios that demand low power operation while maintaining low latency for stochastic flows. Despite these promising early results, in its current form, CaIN has a number of limitations. We discuss these in the following section.

Figure 11 focuses on receiver energy efficiency. If energy consumption in mesh networks were to be driven by transmitter power consumption alone, systems like BLE and SMIP would considerably outperform CaIN: BLE and SMIP transmitters using the same parameters as mentioned above, require 1.76 nJ/bit and 9.19 nJ/bit, respectively, whereas CaIN consumes either 4.48 per bit (in 5 kbps mode) or 9.52 uJ/bit (in 20 kbps mode). CaIN should hence be understood as a radio design optimised for sparse traffic profiles (i.e. low aggregate throughput) that must be delivered with low power consumption and low latency, in which receiver power consumption dominates transmitter power consumption (cf. [3, 12]).

5.5 Limitations

We believe that CaIN offers a novel solution to supporting low latency flows on low power wireless networks. However, the approach has a number of limitations as follows:

(1) *Range:* the most obvious and fundamental limitation of CaIN is the short range of near-field communication. While we believe that there is scope for incremental range extensions for CaIN, these will always be less than offered by standard far-field radios.
(2) *Speed:* while the link-layer throughput of CaIN is competitive with conventional low power wireless networks at 4.9 to 19.8 kbps, the low frequency of the carrier signal, which is necessary to achieve a reasonable near-field range, limits data rates in comparison to higher frequency transmitters.
(3) *Configurability*: To an extent, the results presented in this paper present a false dichotomy between transmitter power, speed and range. At very close ranges, higher transmission speeds are possible and, as can be inferred from Figure 5, a variable power amplifier is likely to result in significant transmitter power savings at intermediate ranges.
(4) *Sub-optimal front end*: The analog front end of CaIN lacks both impedance matching and band-pass filtering. This implies that significant performance gains may yet be achieved by addressing these shortcomings. The results presented in this paper should therefore be viewed as close to a worst-case for the proposed technology.
(5) *Limited testbed evaluation*: We are confident that the latency results presented in Section 5.3.2 will generalise to larger networks as the observed data were essentially deterministic, however a longitudinal study of a larger-scale CaIN test-bed will add vital insights into reliability and robustness that are not captured in the current study.

6 Related Work

CaIN improves the energy-latency trade-offs that characterise low-power networks by introducing the paradigm of near-field mesh networking to support low latency, aperiodic traffic. As will be discussed, several contemporary research lines improve the same trade-off, often introducing some form of network-wide coordination that is highly contingent on existing, far-field PHYsical-layer (PHY) design. CaIN's performance advantages on top of an arguably more primitive network layer hence demonstrate the necessity of

a new physical-layer foundation. In particular, Section 6.1 examines PHY-dependent coordination mechanisms that more efficiently disseminate data. Section 6.2 then focuses on coordination mechanisms that reduce the amount of time nodes spend awake waiting for data that is lost or irrelevant. Still, these mechanisms contribute physical-layer design elements that prove complementary to those covered in this paper. Section 6.3 discusses the extent to which these elements could be reconciled with near-field mesh networking.

6.1 Efficiently Disseminating Data

In duty-cycled networks that route packets along multiple hops, nodes can conserve energy by only waking up when they are part of the routing path. Likewise, if multiple forwarding paths cover a given region of space, the energy burden of active listening can be divided between possible forwarders. Low-power mesh networks hence leave considerable space for cross-layer optimisation [10]. Staffetta [5], for instance, adjusts radio duty cycles in a routing topology-aware fashion. Likewise, so-called Coalesced Intermittency [18] desynchronises the duty cycles of intermittently powered nodes that are deployed close together to provide the illusion of near-continuous availability. Reconciling such *opportunistic* medium access control and routing with ultra low power radio design to further improve energy-latency trade-offs [23] is nevertheless nontrivial: simulation results reveal that principles of "good" radio design subject to microwatt-level power constraints may vary with the routing topology [16] due to the interaction between radio sensitivity and medium access control. Similarly, fast coordinated responses to environmental changes require nodes to have synchronised rather than desynschronised duty cycles [9]. As the runtime optimisation of such conflicting design criteria and mutually interacting network parameters is a considerable challenge itself [8, 44], theses paper leave the study of such cross-layer complexities to future work, instead demonstrating that the physical-layer assumptions on which current studies are based may not be fully justified.

A recent line of research sidesteps the complex interactions between radio design and routing by replacing the latter with *Synchronous Transmissions (ST)*, a technique that efficiently disseminates data through network-wide broadcasts on top of highly parallelised link-layer anycasts, exploiting physical-layer properties to avoid interference between concurrent transmissions [45]. Still, reconciling such efficient dissemination with aperiodic traffic and low average power consumption is nontrivial, since the choice of PHY determines power consumption, the degree of synchronisation enabled by broadcast wake-up signals, and the degree of synchronisation required for ST (cf. [1, 15, 33, 41]). Zippy [33] solves these interconnected problems by introducing an ST-based 434 MHz (far-field) network design based on On-Off Keying, delivering a 2-byte packet across 3 hops in roughly 40 milliseconds, with a per-node power consumption of 8 µW when receiving and 45 mW when transmitting. In scenarios where communication is sparse in time and receiver behaviour dominates average power consumption, this paper hence demonstrates order-of-magnitude power reductions while further reducing latency through appropriate PHY design. Similarly, Radunovic et al. have argued that the adoption of mesh networks relying on carrier frequencies in the 100s of MHz would enable new transmission modalities (i.e. full-duplex wireless) and simplifies cross-layer design concerns [29].

6.2 Sleeping Early and Often

Low-power, low-latency wireless networking requires that nodes sleep as often as possible. Nodes should hence avoid waiting for data that will not arrive and coordinate channel access to prevent wasted listening time due to contention and interference [34]. Blitz [35] hence coordinates access to an ST-based communication channel, starting from 434 MHz WuRs, thus mitigating contention. Similarly, Crystal [12] suppresses irrelevant transmissions; as sensor data evolves according to predictable patterns, data collection applications can suffice with scarce, aperiodic, ST-based updates that indicate when sensor data deviates from its predicted evolution. While such higher-level protocol considerations are not addresses in this paper, recent results highlight the importance of appropriate PHY design in this context as swell, albeit without considering the impact of always-on radios: ST-like broadcasting of ultra-wideband preambles, combined with preamble sampling, energy-efficiently signal the presence or absence of data and hence reduce the energy consumption of the protocols mentioned in this paragraph by enabling early termination of their execution [32].

6.3 Complementary PHY Techniques

State-of-the-art low-power, low-latency mesh networks incorporate several additional physical-layer mechanisms that could further improve this paper's approach. Blitz [35], for example, shows that on-off keyed wake-up signals exhibit temporal features that enable the fast detection of spurious wake-ups using simple classifiers. Structured or modulated preambles can likewise improve performance through hardware-based false-positive wake-up mitigation [25] and thereby help overcome interference [33]. A recent stream of backscatter innovation also shows that CaIN-like envelope detection may achieve hundreds of metres of range under more challenging signal-to-noise regimes than tackled in this paper by using modulated transmissions, but these efforts for now remain limited to transmitters and receivers that consume on the order of one watt and tens of microwatts, respectively [11, 14, 31]. Nevertheless, nearly passive radios should not be expected to achieve data rates and ranges comparable to those of conventional radios due to their lower sensitivity [16]: several of the aforementioned platforms rely on heterogeneous, wake-up radio designs, which switch to a second, faster, more power consuming radio mode after a wake-up phase [3, 27, 35]. Such dual-radio schemes could be built on top of CaIN as future work, though this paper demonstrates that near-field mesh networking already outperforms arguably more optimised, far-field approaches, while introducing considerably less hardware complexity.

For some applications, deployment specifics simplify low-power, low-latency mesh network design. The spatio-temporally correlated way in which seismic events present themselves at distributed sensor nodes, for example, helps coordinate wake-up and data dissemination to further improve power-latency trade-off in mesh networks [3]. Likewise, deployment-specific constraints on network topology simplify the cross-layer design concerns laid out in Section 6.1 [13].

7 Conclusion

This paper introduced CaIN, a novel approach to low-power mesh networking which depends upon near field effects to dramatically

reduce the power of idle listening (558nW). Using CaIN, we introduce a new concept, *near field mesh networking* which offers a unique combination of low power and low latency networking. This is primarily due to CaINs always-on operation, which maintains a per-hop latency under 12ms in all configurations, close to Bluetooth Low Energy (BLE) or 802.15.4/Zigbee at a 100% duty cycle, in which mode these protocols consume thousands of times more energy.

The CaIN transmitter offers two power levels. At 23.5 mW transmit power, CaIN offers 4.9 kbps of link layer throughput, 12.2 ms per-hop latency and 7 m range with over 80% reliability. At 201.7 mW transmit power, CaIN offers 19.8 kbps of link layer throughput, 3.02 ms per-hop latency and 17 m of range at 80% reliability. With the exception of range, these characteristics compare favorably to state-of-the-art networks. We believe that, despite CaINs simple and low-cost transceiver design, the achieved performance envelope points towards a bright future for near-field mesh networking. In the interests of reproducibility, all software and hardware is released open source at https://github.com/KULeuvenNESLFradio/CaIN.

Stepping back from technical specifics, we believe that there CaIN offers one more piece of evidence that novel, clean slate radio designs can significantly improve the performance of resource-constrained wireless networking [7, 37, 42, 43].

8 Future Work

Our future work will proceed along three fronts. A performance-oriented track will explore how to increase the efficiency of the CaIN transmitter, and thereby lower the power consumption of message transmission. While the current hardware implementation is only effective to 20 kbps, initial evidence from lab experiments suggests that link-level data rates of up to 100 kbps may be possible through a redesign of the data slicer sub-system.

The protocol-oriented track of our future work will focus on data link and network layer protocols that exploit the unique near-free listening property of CaIN. The current single-controller bus architecture is rather restrictive and we intend in the future to investigate multi-controller approaches, which will allow any CaIN node to initiate communication. This will necessitate the extension of the CaIN data link layer with contention management techniques such as Carrier Sense Medium Access (CSMA). We will also investigate how existing approaches such as the Routing Protocol for Low-Power and Lossy Networks (RPL) [39] and Ad-Hoc On Demand Distance Vector (AODV) [22] can be applied for static and mobile scenarios respectively.

Finally, in an engineering-oriented track, we will first scale-up the CaIN testbed to 10s of nodes and then explore the extent to which CaIN may be brought into compliance with certification standards for the 40 MHZ VHF radio control band. We also envisage the creation of a dedicated packet-based transciever module, which offers a simplied interface to the application MCU and a greater degree of dynamic transceiver configuration.

Acknowledgment

This work is partially funded by Research Fund KU Leuven, J. Oostvogels' Research Foundation - Flanders fellowship (FWO; 1224325N), the FWO LOCUSTS project (G019722N), and the Horizon Europe OpenSwarm project[9].

References

[1] Michael Baddeley, Carlo Alberto Boano, Antonio Escobar-Molero, Ye Liu, Xiaoyuan Ma, Usman Raza, Kay Römer, Markus Schuß, and Aleksandar Stanoev. 2020. The Impact of the Physical Layer on the Performance of Concurrent Transmissions. In *2020 IEEE 28th International Conference on Network Protocols (ICNP)*. 1–12.

[2] Sadok Bdiri and Faouzi Derbel. 2014. A Nanowatt Wake-Up Receiver for Industrial Production Line. In *2014 IEEE 11th International Multi-Conference on Systems, Signals & Devices (SSD14)*. 1–6.

[3] Andreas Biri, Reto Da Forno, Tonio Gsell, Tobias Gatschet, Jan Beutel, and Lothar Thiele. 2021. STeC: Exploiting Spatial and Temporal Correlation for Event-based Communication in WSNs. In *Proceedings of the 19th ACM Conference on Embedded Networked Sensor Systems (SenSys '21)*. ACM, New York, NY, USA, 274–287.

[4] Michael Buettner, Gary V. Yee, Eric Anderson, and Richard Han. 2006. X-MAC: A Short Preamble MAC Protocol for Duty-Cycled Wireless Sensor Networks. In *Proceedings of the 4th International Conference on Embedded Networked Sensor Systems (SenSys '06)*. ACM, New York, NY, USA, 307–320.

[5] Marco Cattani, Andreas Loukas, Marco Zimmerling, Marco Zuniga, and Koen Langendoen. 2016. Staffetta: Smart Duty-Cycling for Opportunistic Data Collection. In *Proceedings of the 14th ACM Conference on Embedded Network Sensor Systems*. 56–69.

[6] P. Arun Mozhi Devan, Fawnizu Azmadi Hussin, Rosdiazli Ibrahim, Kishore Bingi, and Farooq Ahmad Khanday. 2021. A Survey on the Application of WirelessHART for Industrial Process Monitoring and Control. *Sensors* 21, 15 (2021).

[7] Justin Feng, Timothy Jacques, Omid Abari, and Nader Sehatbakhsh. 2023. Everything has its Bad Side and Good Side: Turning Processors to Low Overhead Radios Using Side-Channels. In *Proceedings of the 22nd International Conference on Information Processing in Sensor Networks (IPSN '23)*. ACM, New York, NY, USA, 288–301.

[8] Federico Ferrari, Marco Zimmerling, Luca Mottola, and Lothar Thiele. 2012. Low-power wireless bus. In *Proceedings of the 10th ACM Conference on Embedded Network Sensor Systems* (Toronto, Ontario, Canada) *(SenSys '12)*. Association for Computing Machinery, New York, NY, USA, 1–14. https://doi.org/10.1145/2426656.2426658

[9] Kai Geissdoerfer and Marco Zimmerling. 2021. Bootstrapping Battery-Free Wireless Networks: Efficient Neighbor Discovery and Synchronization in the Face of Intermittency. In *18th USENIX Symposium on Networked Systems Design and Implementation (NSDI 21)*. 439–455.

[10] Mayssa Ghribi and Aref Meddeb. 2020. Survey and Taxonomy of MAC, Routing and Cross Layer Protocols Using Wake-Up Radio. *Journal of Network and Computer Applications* 149 (2020), 102465.

[11] Xiuzhen Guo, Longfei Shangguan, Yuan He, Nan Jing, Jiacheng Zhang, Haotian Jiang, and Yunhao Liu. 2022. Saiyan: Design and Implementation of a Low-Power Demodulator for LoRa Backscatter Systems. In *19th USENIX Symposium on Networked Systems Design and Implementation (NSDI 22)*. 437–451.

[12] Timofei Istomin, Amy L. Murphy, Gian Pietro Picco, and Usman Raza. 2016. Data Prediction + Synchronous Transmissions = Ultra-low Power Wireless Sensor Networks. In *Proceedings of the 14th ACM Conference on Embedded Network Sensor Systems (SenSys '16)*. ACM, New York, NY, USA, 83–95.

[13] Heikki Karvonen, Juha Petäjäjärvi, Jari Iinatti, Matti Hämäläinen, and Carlos Pomalaza-Ráez. 2014. A Generic Wake-Up Radio Based MAC Protocol for Energy Efficient Short range Communication. In *2014 IEEE 25th Annual International Symposium on Personal, Indoor, and Mobile Radio Communication (PIMRC)*. 2173–2177.

[14] Songfan Li, Hui Zheng, Chong Zhang, Yihang Song, Shen Yang, Minghua Chen, Li Lu, and Mo Li. 2022. Passive DSSS: Empowering the Downlink Communication for Backscatter Systems. In *19th USENIX symposium on networked systems design and implementation (NSDI 22)*. 913–928.

[15] Mengyao Liu, Jonathan Oostvogels, Sam Michiels, Wouter Joosen, and Danny Hughes. 2022. BoboLink: low latency and low power communication for intelligent environments. In *2022 18th International Conference on Intelligent Environments (IE)*. IEEE, 1–4.

[16] Edward Longman, Mohammed El-Hajjar, and Geoff V. Merrett. 2023. Multihop Networking for Intermittent Devices. In *Proceedings of the 20th ACM Conference on Embedded Networked Sensor Systems (SenSys '22)*. ACM, New York, NY, USA, 878–884.

[9]This document is issued within the frame and for the purpose of the OpenSwarm project. This project has received funding from the European Union's Horizon Europe Framework under Grant 101093046. Views and opinions expressed are however those of the author(s) only, and the European Commission is not responsible for any use that may be made of the information it contains.

[17] Michele Magno, Vana Jelicic, Bruno Srbinovski, Vedran Bilas, Emanuel Popovici, and Luca Benini. 2016. Design, Implementation, and Performance Evaluation of a Flexible Low-Latency Nanowatt Wake-Up Radio Receiver. *IEEE Transactions on Industrial Informatics* 12, 2 (2016), 633–644.

[18] Amjad Yousef Majid, Patrick Schilder, and Koen Langendoen. 2020. Continuous Sensing on Intermittent Power. In *2020 19th ACM/IEEE International Conference on Information Processing in Sensor Networks (IPSN)*. 181–192.

[19] Stevan Marinkovic and Emanuel Popovici. 2012. Ultra Low Power Signal Oriented Approach for Wireless Health Monitoring. *Sensors* 12, 6 (2012), 7917–7937.

[20] Stevan J. Marinkovic and Emanuel M. Popovici. 2011. Nano-Power Wireless Wake-Up Receiver With Serial Peripheral Interface. *IEEE Journal on Selected Areas in Communications* 29, 8 (2011), 1641–1647.

[21] Einar Sneve Martinussen and Timo Arnall. 2009. Designing with RFID. In *Proceedings of the 3rd International Conference on Tangible and Embedded Interaction (TEI '09)*. ACM, New York, NY, USA, 343–350.

[22] Razvan Musaloiu-E., Chieh-Jan Mike Liang, and Andreas Terzis. 2008. Koala: Ultra-Low Power Data Retrieval in Wireless Sensor Networks. In *2008 International Conference on Information Processing in Sensor Networks (ipsn 2008)*. 421–432.

[23] Joaquim Oller, Ilker Demirkol, Jordi Casademont, Josep Paradells, Gerd Ulrich Gamm, and Leonhard Reindl. 2015. Has Time Come to Switch from Duty-Cycled MAC Protocols to Wake-Up Radio for Wireless Sensor Networks? *IEEE/ACM Transactions on Networking* 24, 2 (2015), 674–687.

[24] C.E. Perkins and E.M. Royer. 1999. Ad-hoc On-Demand Distance Vector Routing. In *Proceedings WMCSA'99. Second IEEE Workshop on Mobile Computing Systems and Applications*. 90–100.

[25] Chiara Petrioli, Dora Spenza, Pasquale Tommasino, and Alessandro Trifiletti. 2014. A Novel Wake-Up Receiver with Addressing Capability for Wireless Sensor Nodes. In *2014 IEEE International Conference on Distributed Computing in Sensor Systems*. 18–25.

[26] Rajeev Piyare, Amy L. Murphy, Csaba Kiraly, Pietro Tosato, and Davide Brunelli. 2017. Ultra Low Power Wake-Up Radios: A Hardware and Networking Survey. *IEEE Communications Surveys & Tutorials* 19, 4 (2017), 2117–2157.

[27] Rajeev Piyare, Amy L. Murphy, Michele Magno, and Luca Benini. 2018. On-Demand LoRa: Asynchronous TDMA for Energy Efficient and Low Latency Communication in IoT. *Sensors* 18, 11 (2018).

[28] Joseph Polastre, Jason Hill, and David Culler. 2004. Versatile Low Power Media Access for Wireless Sensor Networks. In *Proceedings of the 2nd International Conference on Embedded Networked Sensor Systems (SenSys '04)*. ACM, New York, NY, USA, 95–107.

[29] Bozidar Radunovic, Dinan Gunawardena, Peter Key, Alexandre Proutiere, Nikhil Singh, Vlad Balan, and Gerald Dejean. 2010. Rethinking Indoor Wireless Mesh Design: Low Power, Low Frequency, Full-Duplex. In *2010 Fifth IEEE Workshop on Wireless Mesh Networks*. 1–6.

[30] Alanson P. Sample, Daniel J. Yeager, Pauline S. Powledge, Alexander V. Mamishev, and Joshua R. Smith. 2008. Design of an RFID-Based Battery-Free Programmable Sensing Platform. *IEEE Transactions on Instrumentation and Measurement* 57, 11 (2008), 2608–2615.

[31] Yihang Song, Li Lu, Jiliang Wang, Chong Zhang, Hui Zheng, Shen Yang, Jinsong Han, and Jian Li. 2023. µMote: Enabling Passive Chirp De-spreading and µW-level Long-Range Downlink for Backscatter Devices. In *20th USENIX symposium on networked systems design and implementation (NSDI 23)*. 1751–1766.

[32] Enrico Soprana, Matteo Trobinger, Davide Vecchia, and Gian Pietro Picco. 2023. Network On or Off? Instant Global Binary Decisions over UWB with Flick. In *Proceedings of the 22nd International Conference on Information Processing in Sensor Networks (IPSN '23)*. ACM, New York, NY, USA, 261–273.

[33] Felix Sutton, Bernhard Buchli, Jan Beutel, and Lothar Thiele. 2015. Zippy: On-Demand Network Flooding. In *Proceedings of the 13th ACM Conference on Embedded Networked Sensor Systems (SenSys '15)*. ACM, New York, NY, USA, 45–58.

[34] Felix Sutton, Reto Da Forno, David Gschwend, Tonio Gsell, Roman Lim, Jan Beutel, and Lothar Thiele. 2017. The Design of a Responsive and Energy-efficient Event-triggered Wireless Sensing System.. In *EWSN*. 144–155.

[35] Felix Sutton, Reto Da Forno, Jan Beutel, and Lothar Thiele. 2019. BLITZ: Low Latency and Energy-Efficient Communication for Event-Triggered Wireless Sensing Systems. *ACM Trans. Sen. Netw.* 15, 2, Article 25 (mar 2019), 38 pages.

[36] Ashok Samraj Thangarajan, Thien Duc Nguyen, Mengyao Liu, Sam Michiels, Fan Yang, Ka Lok Man, Jieming Ma, Wouter Joosen, and Danny Hughes. 2022. Static: Low Frequency Energy Harvesting and Power Transfer for the Internet of Things. *Frontiers in Signal Processing* 1 (2022).

[37] Ambuj Varshney, Wenqing Yan, and Prabal Dutta. 2022. Judo: Addressing the Energy Asymmetry of Wireless Embedded Systems Through Tunnel Diode Based Wireless Transmitters. In *Proceedings of the 20th Annual International Conference on Mobile Systems, Applications and Services (MobiSys '22)*. ACM, New York, NY, USA, 273–286.

[38] Xavier Vilajosana, Thomas Watteyne, Tengfei Chang, Mališa Vučinić, Simon Duquennoy, and Pascal Thubert. 2020. IETF 6TiSCH: A Tutorial. *IEEE Communications Surveys & Tutorials* 22, 1 (2020), 595–615.

[39] Thomas Watteyne, Lance Doherty, Jonathan Simon, and Kris Pister. 2013. Technical Overview of SmartMesh IP. In *2013 Seventh International Conference on Innovative Mobile and Internet Services in Ubiquitous Computing*. 547–551.

[40] Tim Winter. [n. d.]. RFC 6550: RPL: IPv6 Routing Protocol for Low-Power and Lossy Networks — datatracker.ietf.org. _url-https://datatracker.ietf.org/doc/html/rfc6550. [Accessed 02-05-2024].

[41] Fan Yang, Jonathan Oostvogels, Sam Michiels, and Danny Hughes. 2020. Achieving Deterministic and Low-Latency Wireless Connection with Zero-Wire: Demo Abstract. In *Proceedings of the 18th Conference on Embedded Networked Sensor Systems (SenSys)*. ACM, 591–592.

[42] Junbo Zhang, Elahe Soltanaghai, Artur Balanuta, Reese Grimsley, Swarun Kumar, and Anthony Rowe. 2022. PLatter: On the Feasibility of Building-scale Power Line Backscatter. In *19th USENIX Symposium on Networked Systems Design and Implementation (NSDI 22)*. 897–911.

[43] Renjie Zhao, Kejia Wang, Kai Zheng, Xinyu Zhang, and Vincent Leung. 2023. SlimWiFi: Ultra-Low-Power IoT Radio Architecture Enabled by Asymmetric Communication. In *20th USENIX Symposium on Networked Systems Design and Implementation (NSDI 23)*. 1201–1219.

[44] Marco Zimmerling, Federico Ferrari, Luca Mottola, Thiemo Voigt, and Lothar Thiele. 2012. pTunes: Runtime Parameter Adaptation for Low-Power MAC protocols. In *Proceedings of the 11th International Conference on Information Processing in Sensor Networks (IPSN '12)*. ACM, New York, NY, USA, 173–184.

[45] Marco Zimmerling, Luca Mottola, and Silvia Santini. 2020. Synchronous Transmissions in Low-Power Wireless: A Survey of Communication Protocols and Network Services. *ACM Comput. Surv.* 53, 6, Article 121 (dec 2020), 39 pages.